



DTI of the kidney in children: comparison between normal kidneys and those with ureteropelvic junction (UPJ) obstruction

Hansel J. Otero¹ · Juan S. Calle-Toro¹ · Carolina L. Maya¹ · Kassa Darge¹ · Suraj D. Serai¹

Received: 2 July 2019 / Revised: 25 November 2019 / Accepted: 30 November 2019 / Published online: 16 December 2019
© European Society for Magnetic Resonance in Medicine and Biology (ESMRMB) 2019

Abstract

Objective To compare renal diffusion tensor imaging (DTI) parameters in patients with or without ureteropelvic junction (UPJ) obstruction.

Methods Patients that underwent functional MR urography (MRU) with renal DTI were retrospectively selected. Kidneys deemed normal on T2-weighted images and functional parameters were used as controls and compared to those kidneys with morphologic and functional findings of UPJ obstruction. DTI included a 20-direction DTI with b values of $b=0$ s/mm² and $b=400$ s/mm². Diffusion Toolkit was used for analysis and segmentation. TrackVis was used to draw regions of interest (ROI) covering the entire volume of the renal parenchyma, excluding the collecting system. Fibers were reconstructed using a deterministic fiber tracking algorithm. Whole kidney ROI-based analysis was performed to obtain cortico-medullary measurements (FA, ADC and track length) for each kidney. T tests were performed to compare means and statistical significance was defined at $p < 0.05$.

Results 118 normal kidneys from 102 patients (median age 7 years, IQR 6–15 years; 58 males and 44 females) were compared to 22 kidneys from 16 patients (median age 13 years, IQR 3–15 years; 9 males and 7 females) with UPJ obstruction. Mean FA values were significantly lower (0.31 ± 0.07 ; $n = 22$) in kidneys with UPJ obstruction than normal kidneys (0.40 ± 0.08 ; $n = 118$) ($p < 0.001$). ADC was marginally significantly increased ($p = 0.01$) and track length was not significantly different ($p = 0.24$).

Conclusion Our results suggest that DTI-derived metrics including FA and ADC are potential biomarkers to differentiate kidneys with UPJ obstruction and assess renal parenchymal damage.

Keywords Diffusion tensor imaging · Magnetic resonance imaging · Ureteropelvic junction obstruction · Renal DTI · UPJ

Introduction

Ureteropelvic junction (UPJ) obstruction is blockage of the flow of urine that occurs where the renal pelvis joins the ureter, which can be congenital or acquired. The most probable cause of congenital UPJ obstruction is failure in development of the renal pelvis–ureter junction or impaired smooth muscle differentiation [1]. However, it could also be due to other causes such as obstructing stones or extrinsic, as for example, an aberrant or accessory renal artery or arterial

branch crossing the lower pole of the kidney, resulting in compression of the UPJ and blockage of urinary flow [2]. Urinary tract dilatation (UTD) is the most common congenital anomaly identified prenatally, being present in 1–3% of pregnancies [3]. While the majority of UTD cases are transient or physiologic and do not require additional interventions (41–88%), UPJ obstruction is the most common pathologic cause [4], explaining 10–30% of cases of UTD in infants (approximately 1 in 1000–1500 live births) [3, 5–7]. This condition affects more boys than girls and is more common in the left kidney but can be bilateral in over 25% of cases [8].

Although ultrasonography is the first image modality used to assess urinary tract dilatation, functional magnetic resonance urography (fMRU) has the ability to better delineate the urinary tract anatomy, help define the point of obstruction, determine the relative renal function and simulate the

✉ Suraj D. Serai
serais@email.chop.edu

¹ Department of Radiology, The Children's Hospital of Philadelphia, University of Pennsylvania School of Medicine, 3401 Civic Center Blvd., Philadelphia, PA 19104, USA

diuretic renogram by providing washout data [9–14]. In particular, both the nuclear medicine diuretic renograms and fMRU, assuming proper positioning and technique, provide useful information for differentiating patients with equivocal UPJ obstruction. If a system is dilated but not obstructed, it responds to diuretics resulting in rapid “wash out” of radiotracer or contrast, while a genuinely obstructed system will show impaired flow regardless of the urinary flow rate [15].

Diffusion tensor imaging (DTI) is based on the application of diffusion gradients in different directions in space, enabling the evaluation of the movement of water molecules in 3D and whether there is a dominant direction to diffusion restriction, which allows to determine fiber tracts according to the dominant direction of water movement in each voxel [16–18]. DTI provides several quantitative parameters including fractional anisotropy (FA), apparent diffusion coefficient (ADC) and also allows to generate tractography maps [16]. FA reflects on how dominant one particular water movement direction in a voxel is and is measured from 0 to 1, while ADC measures the directionally averaged diffusivity [17]. The use of DTI for evaluation of the kidneys has been reported in adults with chronic kidney disease [19, 20] as well as in children with ARPKD [21] and in a small cohort of patients with urinary tract dilatation [18]. The idea is to use quantitative parameters derived from DTI to monitor microstructural changes, which could help differentiate between capacious and obstructed systems and if so, provide additional information to instruct the time for intervention. Hence, our objective was to compare renal DTI parameters in normal kidneys against those with UPJ obstruction.

Methods

The institutional review board at our hospital approved this retrospective Health Insurance Portability and Accountability Act (HIPAA)-compliant study. Between August 2014 and February 2018, patients that underwent fMRU and included DTI were identified. All studies were performed on a 1.5 T magnet (Avanto[®], Siemens). All patients had received intravenous hydration (20 ml/kg) over an hour prior to the exam and furosemide (1 mg/kg; maximum 20 mg) right before localizers (approximately 20 min before contrast administration). All patients had a bladder catheter in place for the study, which is open and draining by gravity during dynamic post-contrast image acquisition to decompress the bladder and avoid confounding factors such as increased retrograde pressure and vesicoureteral reflux. Briefly, the fMRU protocol included axial T2-weighted (TR: 4000 ms, TE: 85 ms), coronal heavily T2-weighted (TR: 6000 ms, TE: 600 ms) as well as pre- and dynamic post-contrast T1 GRE (TR: 3.6 ms, TE: 1.2 ms). The dynamic post-contrast images were obtained at 10 s intervals over 8 min. A gadolinium-based

contrast agent was administered at a rate of 0.1 ml/s using standard dose (0.1 mmol/kg). Post-contrast images were post-processed to calculate functional parameters including differential renal function, calyceal transit time (i.e., time from contrast arrival into the abdominal aorta to contrast seen in the collecting system), and renal transit time (i.e., time from contrast arrival into the abdominal aorta to contrast clearance into the ureter below the lower pole of the kidney). All fMRU post-processing analyses were carried out with publicly available software (<https://www.chop-fmru.com>).

Kidneys deemed morphologically normal on T2-weighted images (i.e., normal size for age, subjectively maintained cortico-medullary differentiation, and absence of focal lesions, cysts or pelvicalyceal dilatation) and with normal functional parameters in dynamic contrast T1-weighted images (including calyceal and renal transit time under 4 min., and an even differential function based on volume), were used as controls [12] and compared to those kidneys with morphologic and functional features of UPJ obstruction. UPJ obstruction was defined in those kidneys with central and peripheral calyceal dilatation as well as a dilated renal pelvis with point of transition at the UPJ and abnormal functional parameters including a renal transit time of over 8 min [22].

Diffusion tensor imaging

DTI included a 20-direction acquisition with b values of $b=0$ s/mm² and $b=400$ s/mm² (Table 1). Diffusion Toolkit was used for analysis and segmentation [21].

DTI post-processing

Fibers were reconstructed using a deterministic fiber tracking algorithm. Analysis was performed to obtain

Table 1 Acquisition parameters for DTI

MRI parameters	Values
TR (ms)	2600
TE (ms)	74
Slice thickness (mm)	4
Matrix size	128 × 96
Bandwidth (Hz/pixel)	1698
No. of directions	20
B values (s/mm ²)	0, 400
No. of averages	2
Fat suppression	SPAIR

DTI diffusion tensor imaging, TR relaxation time, TE echo time, ms milliseconds, mm millimeters, SPAIR spectral adiabatic inversion recovery

cortico-medullary measurements (FA, ADC and track length) for each kidney. A post-doctoral fellow with 2 years of experience in DTI research used TrackVis to draw regions of interest (ROI) covering the entire volume of the renal parenchyma, excluding the collecting system by evaluating the DWI images, ADC and FA maps (Fig. 1). These images were used to avoid problems of alignment related to patient motion in between sequences. In patients with UPJ obstruction, care was taken to avoid regions of dilatation. The ADC and FA values based on the ROI data, and the mean length of the tracks based on the fiber track data were exported. An additional ROI in the mid-axial plane of each kidney was drawn for qualitative evaluation of the scalar FA tractography maps.

The fiber tracks obtained from the ROIs were qualitatively analyzed for: tractography quality, direction of tracks and differences in fractional anisotropy within the renal parenchyma. This assessment was done using two tractography maps: (1) a standard color-coded reconstruction to visualize the orientation of tracks where blue tracks represented diffusion in the cranio-caudal direction, green tracks characterized diffusion in the antero-posterior direction and red tracks showed diffusion in the transverse direction (Fig. 2), and (2) a scalar FA map with minimum and maximum FA thresholds of 0.1 and 0.6, respectively, and a maximum turning angle threshold of 55° between two adjacent voxels was

used. Tractography was reconstructed using a deterministic fiber tracking algorithm.

Statistical analysis

Statistical analyses were performed using MedCalc version 18.2 (MedCalc Software, Ostend, Belgium). For the descriptive analysis absolute distributions, percentages and means, standard deviations, medians and ranges were calculated. To evaluate differences in the distribution of nominal data, *t* tests were performed to compare means and statistical significance was defined at $p < 0.05$.

Results

A total of 427 MRUs were screened, resulting in a total of 118 normal kidneys, from 102 patients (median age 7 years, interquartile range (IQR) 6–15 years; 58 males and 44 females) (Table 2). These 118 renal units were compared to 22 kidneys, from 16 patients (median age 13 years, IQR 3–15 years; 9 males and 7 females), with UPJ obstruction (Figs. 3, 4). Of all 118 patients in the final sample, the most common primary indication for fMRU was suspected obstruction (i.e., worsening ultrasound dilatation and/or flank pain) at the UPJ ($n=40$, 33.9%) or at the UVJ ($n=8$,

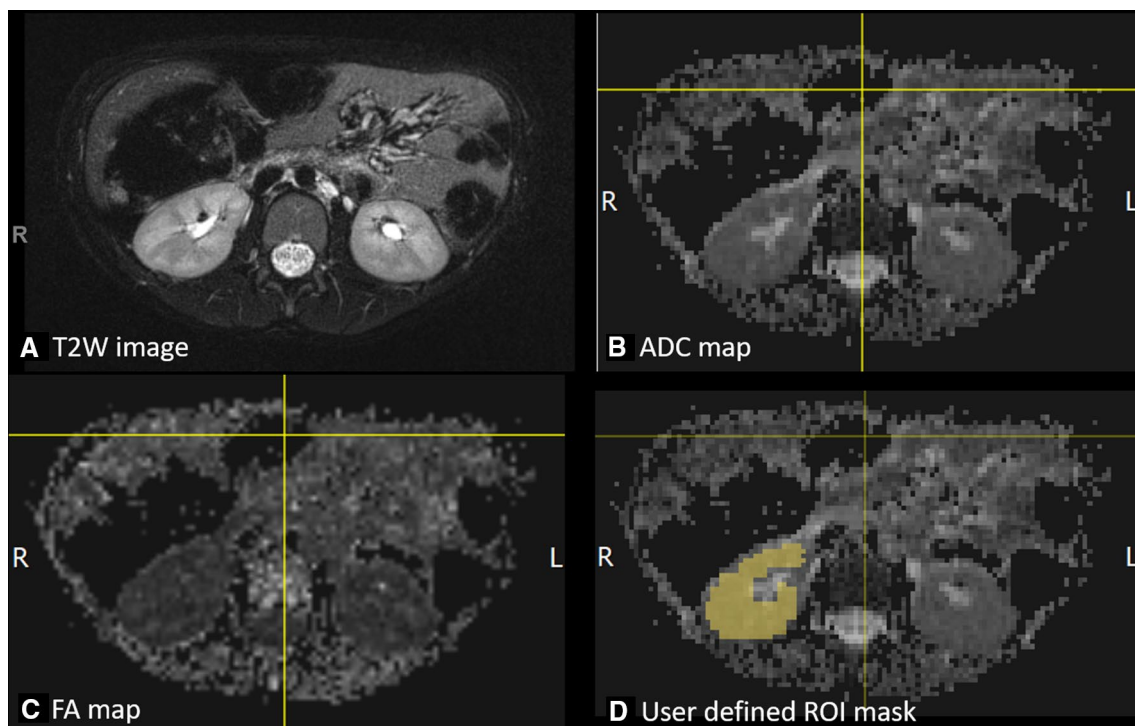


Fig. 1 **a** T2W anatomical image, **b** diffusion-generated ADC map, **c** generated FA map, **d** representative single slice user-defined ROI mask. This patient was a 6 year old girl presented with urinary incon-

tinence to evaluate anatomy. A standard MR urogram study was performed and normal morphology and function were ascertained

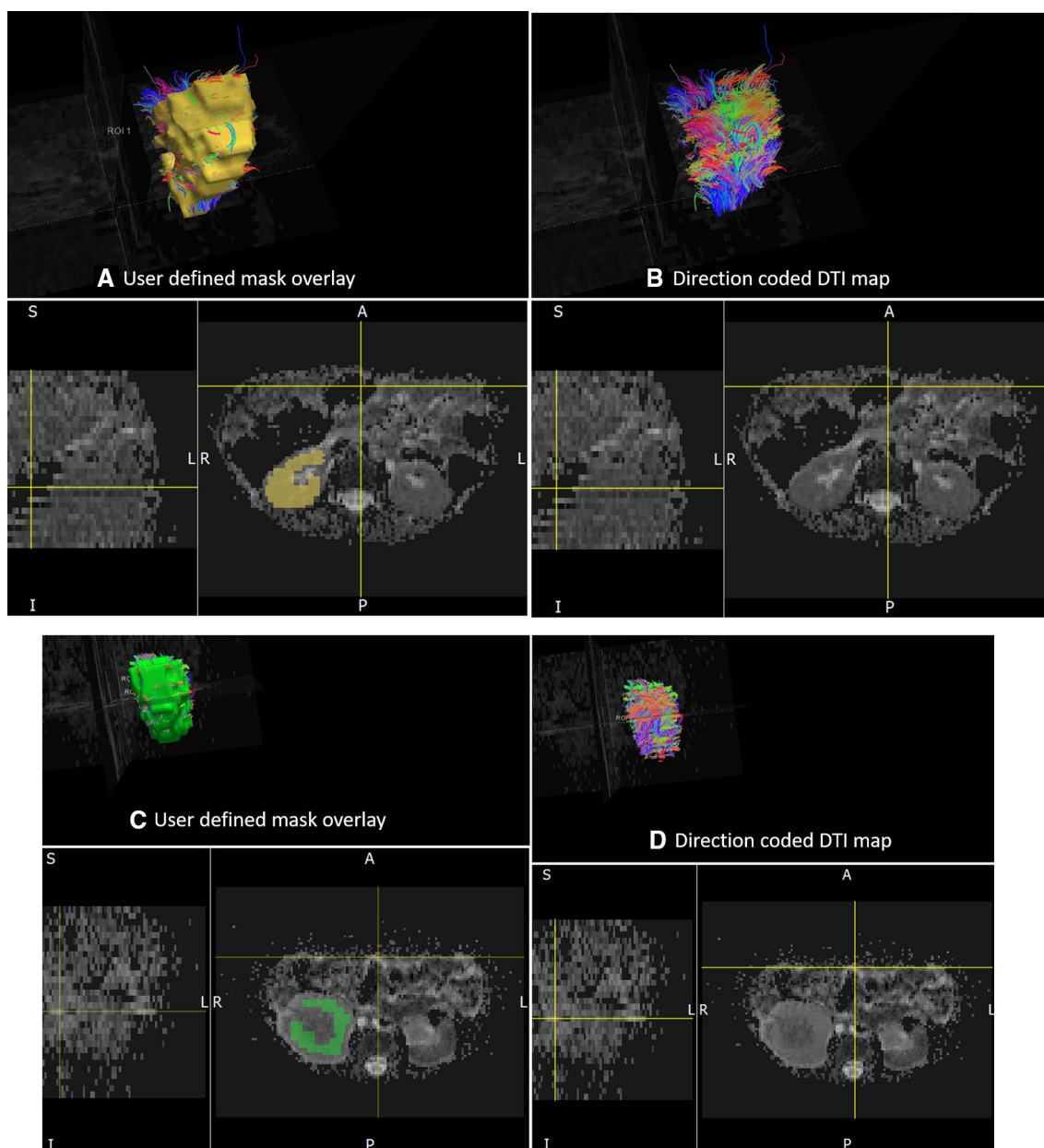


Fig. 2 Representative images of **a** whole kidney overlay with ROI mask and **b** whole kidney direction coded DTI map from a patient with normal kidney; **c** whole kidney overlay with ROI mask and **d** whole kidney direction coded DTI map from a patient with UPJO kidney

Table 2 Subjects' characteristics

Characteristic	Healthy kidneys ($n=118$)	Kidneys with UPJ obstruction ($n=22$)	p value
Age (median, IQR; years)	7.0 (IQR 6–15)	13.0 (IQR 3–15)	0.08
Males, n (%)	58 (56.8%)	9 (56.2%)	n/a

IQR interquartile range, UPJ ureteropelvic junction

6.8%), totaling 48 patients; followed by post-operative evaluation (e.g., pyeloplasty, cyst incision, or ureteral reimplantation) ($n=25$, 21.2%), suspected ectopic ureter ($n=18$,

15.3%), and further characterization of cystic lesion (i.e., suspected calyceal diverticulum) ($n=14$, 33.9%). Other indications included vesicoureteral reflux ($n=4$), febrile urinary

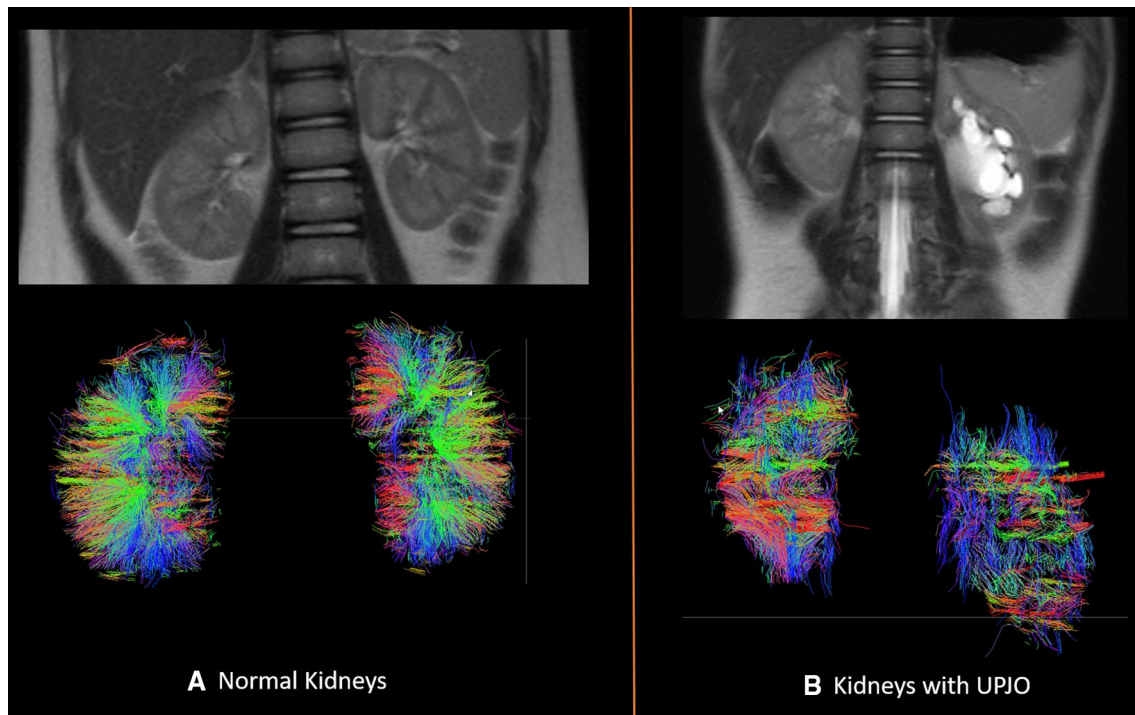


Fig. 3 Representative images from **a** healthy kidney vs **b** patient with unilateral UPJ obstruction

tract infections ($n=3$), history of renal stones ($n=2$), duplex collecting system ($n=2$), multicystic dysplastic kidney ($n=1$) and ureterocele ($n=1$). The subgroup with bilateral normal kidneys ($n=16$) was composed of 14 patients under evaluation for suspected ectopic ureter (e.g., incontinence or continuous wetting) and 2 patients with febrile urinary tract infection.

The mean FA value (mean: $0.31 \pm \text{SD: } 0.07$) in kidneys with UPJ obstruction was significantly lower compared to normal kidneys (0.40 ± 0.08 ; $p < 0.001$) (Fig. 5a). ADC values (mean: $2.58 \pm \text{SD: } 0.37 \times 10^{-3} \text{ mm}^2/\text{s}$) in kidneys with UPJ obstruction were higher than in normal kidneys (mean: $2.25 \pm \text{SD: } 0.39 \times 10^{-3} \text{ mm}^2/\text{s}$; $p=0.01$) (Fig. 5b). The track length was not significantly different between kidneys with UPJ obstruction and normal kidneys (mean $15.39 \pm 7.05 \text{ mm}$ and $11.71 \pm 6.91 \text{ mm}$, respectively; $p=0.24$) (Table 3). A summary of DTI-derived parameters separated by normal kidneys, unilateral ‘healthy kidneys’ from the normal side, kidneys with UPJ obstruction, and unilateral ‘healthy kidneys’ of patients with UPJ obstruction is presented in Table 4.

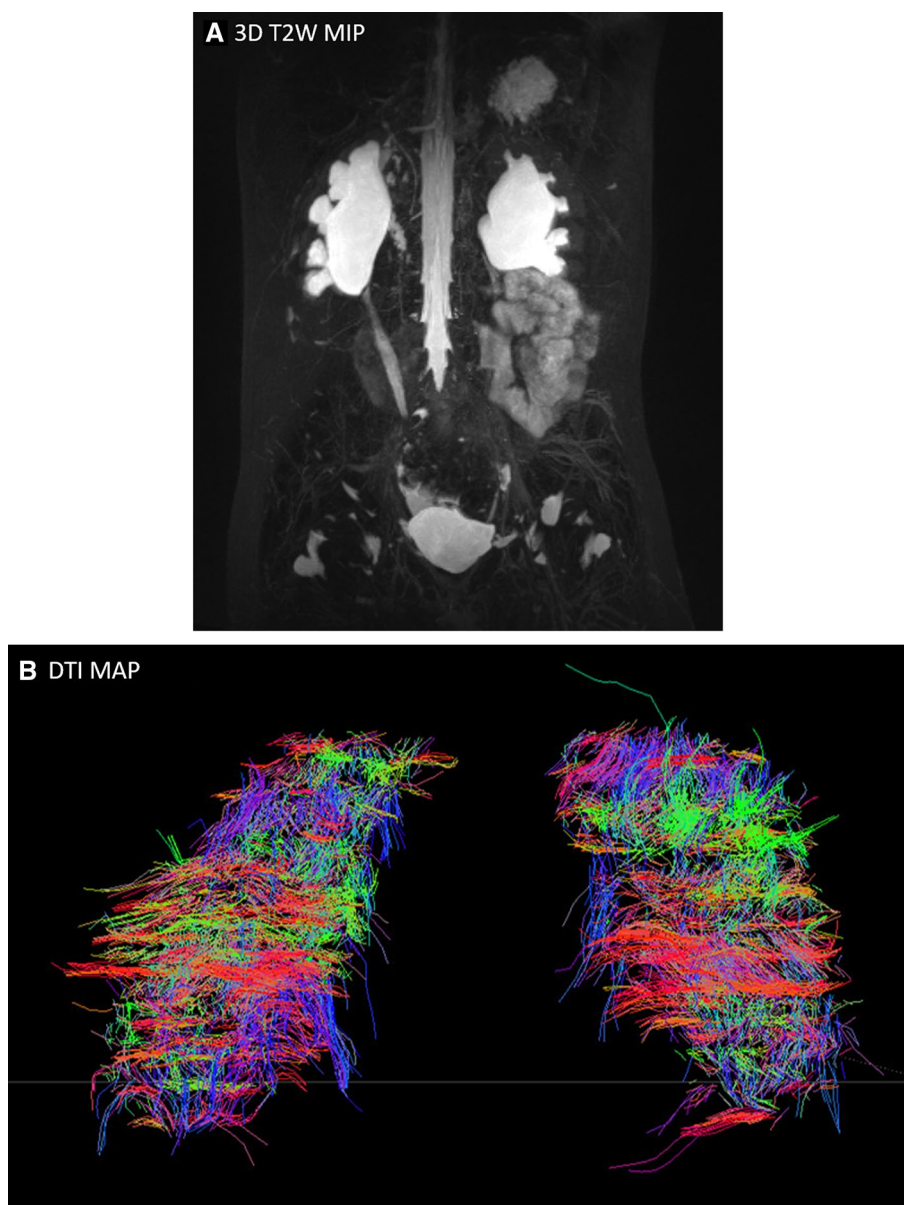
Discussion

We found that DTI-derived FA and ADC values are significantly different between normal kidneys and those with UPJ obstruction. These finding is encouraging because traditional

functional parameters from MRU depend on the administration of gadolinium contrast agents, and the potential risk associated with it, as well as a more lengthy acquisition. However, there was also considerable overlap of the FA and ADC values between the groups, suggesting a larger sample and alternative study designs might be needed before the information can be used clinically. This study is not a direct comparison between the traditionally used $T1/2 > 20 \text{ min}$ on nuclear medicine MAG3 renal scans [23] nor does it attempt to substitute other valuable information derived from post-contrast images on fMRU. The overlap between normal and obstructed kidneys values is also similar to inconclusive values from MAG3 renal scans ($T1/2 > 10$ but $< 20 \text{ min}$) or renal transit time between 4 and 8 min during fMRU [12, 24]. Hence, additional research would be needed to determine the ideal balance between increased sensitivity and improved specificity. In addition, our study does not address individual’s changes in DTI-derived parameters over time, which will be needed if FA and ADC are to be used for monitoring structural changes overtime.

It is important to highlight that, likely as a reflection of our institution’s practice environment, the ages both for patients with UPJ obstruction (median 13 years) and those with normal kidneys (median 7 years) were much older than anticipated for a frequently prenatally diagnosed abnormality. However, while intrinsic causes of UPJ obstruction present early in life, extrinsic causes, including crossing vessels, usually present symptomatically in older

Fig. 4 **a** MIP of 3D T2W acquisition of a 7-year-old boy having UPJO in both kidneys and **b** direction coded DTI map



children. Moreover, fMRU is frequently obtained in the setting of pre-surgical evaluation, which tends to happen later in life. For example, a recent review (laparoscopic transposition of lower pole crossing vessels (vascular hitch) in children with pelviureteric junction obstruction of 51 children undergoing laparoscopy for treatment of UPJ obstruction had a median age of 10.7 years [25]. Similarly, another review of 59 patients with UPJ obstruction had a mean age of 8.1 (range 1.6–18.9) years [26]. Conversely, the cases diagnosed prenatally, including those with normal anatomy and with less than 10–15% relative function, were treated either conservatively or with nephrectomy, purely based on the presence or absence of complications such as febrile urinary tract infections, much earlier in life [27].

DTI metrics help provide rotationally invariant indices that describe the properties of the diffusion profile [17]. The amount of diffusion is characterized by ADC and the anisotropy of diffusion is characterized by FA. FA is a normalized, dimensionless index that measures the properties of anisotropy of DTI [28]. Low FA values imply similar diffusion along all directions, while higher FA implies that there is a marked directional dependence such that diffusion occurs preferentially along one dominant direction. In our sample, FA values tended to be significantly lower in patients with UPJ obstruction as compared to healthy kidneys, which might be related to the loss of the relative unidirectionality of fluid within the nephron during the filtration and excretion processes. Hypothetically, multidirectionality of water diffusion might be

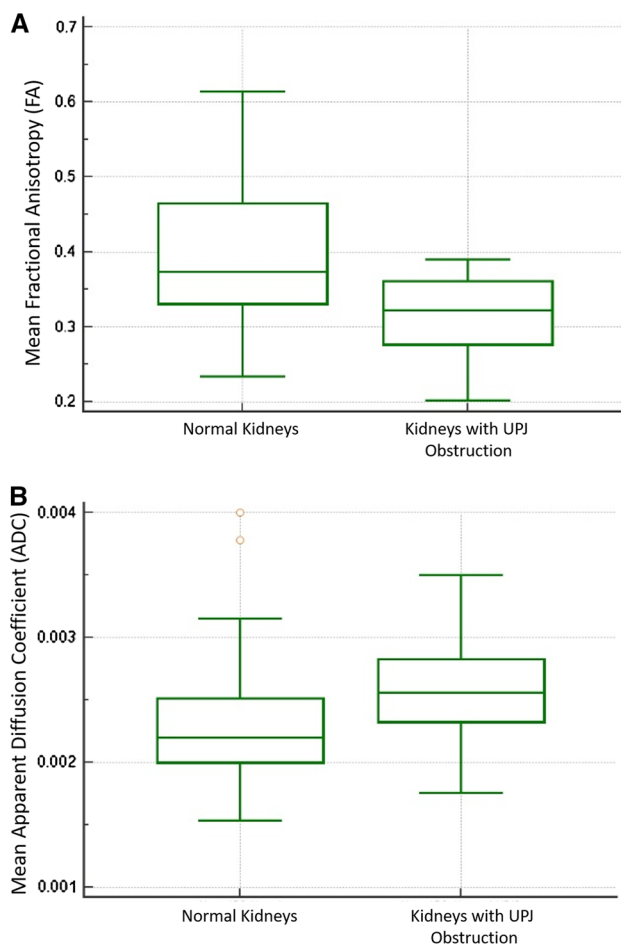


Fig. 5 Box and whisker plot of **a** mean FA and **b** mean ADC in controls vs patients with UPJ obstruction. Horizontal lines within boxes represent medians, and vertical lines and whiskers represent the lowest and highest observations within 1.5 interquartile range of lower and upper quartiles, respectively. The data points with the circles are values that fall outside the 1.5 interquartile range but within 3 interquartile range

Table 3 Kidney DTI parameters in healthy kidneys vs kidneys with UPJ obstruction

DTI parameter (mean \pm SD)	Healthy kidneys (n = 118)	Kidneys with UPJ obstruction (n = 22)	p value
Mean FA	0.40 \pm 0.08	0.31 \pm 0.07	< 0.001
Mean ADC (mm ² /s) $\times 10^{-3}$	2.25 \pm 0.39	2.58 \pm 0.37	0.01
Mean track length (mm)	11.71 \pm 6.91	15.39 \pm 7.05	0.24

UPJ ureteropelvic junction, DTI diffusion tensor imaging

due to one or a combination of several factors including breakage of normal membranous planes, parenchymal edema and interstitial space, also called “third spacing”, slower filtration and excretion rates in affected kidneys,

and/or intraparenchymal reflux in a system under pressure. Another factor that is likely to contribute to the difference in FA is the fact that all MRU images are acquired after the administration of intravenous fluids and diuretics. Diuresis, resulting in an increased urine production, leads to an accumulation of tracer in the parenchyma during diuresis nephrography (nuclear medicine studies) in kidneys with UPJ obstruction, while in normal kidneys diuresis results in a much faster washout as the filtration rate increased from 1 to 3 ml/min to an average of 24 ml/min [29]. Our findings are in accordance to a similar study with a much smaller cohort of only 19 children [30]. Using DTI, a tractography map can also be generated (Figs. 3, 4). Although its exact clinical impact is unclear at this time, the map allows a visualized disruption of the regular arrangement of the tracts in a patient with renal function alteration.

For the ADC values, we demonstrated an increase in the ADC values in kidneys with UPJ obstruction. A study by Hueper et al. [31] found an increase of 10% in ADC values for the transplanted kidneys in relation to healthy control kidneys, which is similar to our findings. Another study by Lanzman et al. [32] found a correlation between glomerular filtration rate and FA values suggesting that DTI derived metrics could be more sensitive in detecting changes in the microstructure earlier than DWI. Wang et al. [33] found that even in patients with chronic kidney disease, ADC values differ among the kidneys with early stages of disease compared to more advanced stages. In a recent work done on 35 children, for 70 kidneys (40 with pelvicalyceal dilation and 30 without pelvicalyceal dilation), renal ADC did not correlate with pelvicalyceal dilation due to suspected or known UPJ obstruction [34]. However, compared to FA, ADC values reported in literature had a higher variability [35], and might be difficult to reproduce.

Our subgroup analysis presented in Table 4 shows decreased mean FA in the two groups of patients with unilateral normal kidneys (0.36 \pm 0.06 in patients with unilateral normal kidneys and 0.31 \pm 0.07 in unilateral ‘healthy’ kidneys of patients with UPJ obstruction) as compared to patients with both normal kidneys, 0.50 \pm 0.06. Mean FA value further decreased in kidneys with UPJ obstruction (0.31 \pm 0.07).

Conclusion

Our results suggest that DTI-derived metrics including FA and ADC are potential biomarkers to differentiate kidneys with UPJ obstruction and assess renal parenchymal damage.

Table 4 Summary of kidney DTI-derived parameters across patient population

DTI parameter (mean \pm SD)	Patients with both kidneys normal	Unilateral 'healthy kidneys' normal side	Kidneys with UPJ obstruction	Unilateral 'healthy kidneys' of patients with UPJ obstruction
Number of patients	16	86	16	10
Number of kidneys	32	86	22	10
Age (median, IQR; years)	8.5 (IQR 7–13)	7.0 (IQR 3–13)	12.9 (IQR 3–15)	9.0 (IQR 4–15)
Males, n (%)	3/16	55/86	9/16	6/10
Mean FA	0.50 \pm 0.06	0.36 \pm 0.06	0.31 \pm 0.07	0.35 \pm 0.03
Mean ADC (mm ² /s) $\times 10^{-3}$	2.32 \pm 0.43	2.23 \pm 0.33	2.58 \pm 0.37	2.22 \pm 0.33
Mean track length (mm)	8.80 \pm 2.64	11.66 \pm 3.21	15.39 \pm 7.05	11.65 \pm 3.21

DTI diffusion tensor imaging, UPJ ureteropelvic junction, SD standard deviation, FA fractional anisotropy, ADC apparent diffusion coefficient, mm millimeter

Funding None.

Compliance with ethical standards

Conflict of interest The authors declare that they no competing interest.

Ethical approval All procedures performed in studies involving human participants were in accordance with the ethical standards of the institutional and/or national research committee and with the 1964 Helsinki Declaration and its later amendments or comparable ethical standards. The institutional review board at our hospital approved this retrospective Health Insurance Portability and Accountability Act (HIPAA)-compliant study. A statement has been included in the methods section of the manuscript.

References

- Klein J, Gonzalez J, Miravete M et al (2011) Congenital ureteropelvic junction obstruction: human disease and animal models. *Int J Exp Pathol* 92(3):168–192
- Lam JS, Breda A, Schulam PG (2007) Ureteropelvic junction obstruction. *J Urol* 177(5):1652–1658
- Balthazar A, Herndon CDA (2018) Prenatal urinary tract dilatation. *Urol Clin N Am* 45(4):641–657
- Tubre RW, Gatti JM (2015) Surgical approaches to pediatric ureteropelvic junction obstruction. *Curr Urol Rep* 16(10):72
- Liang CC, Cheng PJ, Lin CJ, Chen HW, Chao AS, Chang SD (2002) Outcome of prenatally diagnosed fetal hydronephrosis. *J Reprod Med* 47(1):27–32
- Chang CP, McDill BW, Neilson JR et al (2004) Calcineurin is required in urinary tract mesenchyme for the development of the pyeloureteral peristaltic machinery. *J Clin Invest* 113(7):1051–1058
- Josephson S (2002) Antenatally detected, unilateral dilatation of the renal pelvis: a critical review. 1. Postnatal non-operative treatment 20 years on—is it safe? *Scand J Urol Nephrol* 36(4):243–250
- Dhillon HK (1998) Prenatally diagnosed hydronephrosis: the Great Ormond Street experience. *Br J Urol* 81(Suppl 2):39–44
- McDaniel BB, Jones RA, Scherz H, Kirsch AJ, Little SB, Grattan-Smith JD (2005) Dynamic contrast-enhanced MR urography in the evaluation of pediatric hydronephrosis: part 2, anatomic and functional assessment of ureteropelvic junction obstruction (corrected). *AJR Am J Roentgenol* 185(6):1608–1614
- Jones RA, Easley K, Little SB, Scherz H, Kirsch AJ, Grattan-Smith JD (2005) Dynamic contrast-enhanced MR urography in the evaluation of pediatric hydronephrosis: part 1, functional assessment. *AJR Am J Roentgenol* 185(6):1598–1607
- McMann LP, Kirsch AJ, Scherz HC et al (2006) Magnetic resonance urography in the evaluation of prenatally diagnosed hydronephrosis and renal dysgenesis. *J Urol* 176(4 Pt 2):1786–1792
- Dickerson EC, Dillman JR, Smith EA, DiPietro MA, Lebowitz RL, Darge K (2015) Pediatric MR urography: indications, techniques, and approach to review. *Radiographics* 35(4):1208–1230
- Leyendecker JR, Barnes CE, Zagoria RJ (2008) MR urography: techniques and clinical applications. *Radiographics* 28(1):23–46 (**discussion-7**)
- Jones RA, Grattan-Smith JD, Little S (2011) Pediatric magnetic resonance urography. *J Magn Reson Imaging* 33(3):510–526
- Brown SCW (2006) Chapter 9: The urologist's view. In: Alain Prigent MD, Amy Piepsz MD (eds) *Functional Imaging in Nephro-Urology*. Taylor & Francis Abingdon, Oxon UK, pp 67–80
- Notohamprojo M, Reiser MF, Sourbron SP (2010) Diffusion and perfusion of the kidney. *Eur J Radiol* 76(3):337–347
- Hagmann P, Jonasson L, Maeder P, Thiran JP, Wedeen VJ, Meuli R (2006) Understanding diffusion MR imaging techniques: from scalar diffusion-weighted imaging to diffusion tensor imaging and beyond. *Radiographics* 26(Suppl 1):S205–S223
- Jaimes C, Darge K, Khrichenko D, Carson RH, Berman JI (2014) Diffusion tensor imaging and tractography of the kidney in children: feasibility and preliminary experience. *Pediatr Radiol* 44(1):30–41
- Hueper K, Khalifa AA, Brasen JH et al (2016) Diffusion-weighted imaging and diffusion tensor imaging detect delayed graft function and correlate with allograft fibrosis in patients early after kidney transplantation. *J Magn Reson Imaging* 44(1):112–121
- Gaudiano C, Clementi V, Busato F et al (2013) Diffusion tensor imaging and tractography of the kidneys: assessment of chronic parenchymal diseases. *Eur Radiol* 23(6):1678–1685
- Serai SD, Otero HJ, Calle-Toro JS, Berman JI, Darge K, Hartung EA (2019) Diffusion tensor imaging of the kidney in healthy controls and in children and young adults with autosomal recessive polycystic kidney disease. *Abdom Radiol (New York)* 44:1867–1872
- Jones RA, Perez-Brayfield MR, Kirsch AJ, Grattan-Smith JD (2004) Renal transit time with MR urography in children. *Radiology* 233(1):41–50

23. O'Reilly PH (2003) Standardization of the renogram technique for investigating the dilated upper urinary tract and assessing the results of surgery. *BJU Int* 91(3):239–243
24. von Rundstedt FC, Scovell JM, Bian SX, Lee D, Mayer WA, Link RE (2017) Percent of tracer clearance at 40 minutes in MAG3 renal scans is more sensitive than T1/2 for symptomatic ureteropelvic junction obstruction. *Urology* 103:245–250
25. Esposito C, Bleve C, Escolino M et al (2016) Laparoscopic transposition of lower pole crossing vessels (vascular hitch) in children with pelviureteric junction obstruction. *Transl Pediatr* 5(4):256–261
26. Lam PN, Wong C, Mulholland TL, Campbell JB, Kropp BP (2007) Pediatric laparoscopic pyeloplasty: 4-year experience. *J Endourol* 21(12):1467–1471
27. Gopal M, Peycelon M, Caldamone A et al (2019) Management of ureteropelvic junction obstruction in children—a roundtable discussion. *J Pediatr Urol* 15(4):322–329
28. Basser PJ, Pierpaoli C (1996) Microstructural and physiological features of tissues elucidated by quantitative-diffusion-tensor MRI. *J Magn Reson Ser B* 111(3):209–219
29. Piepsz APA (2006) Functional imaging in nephro-urology adults and children. *Functional Imaging in Nephro-Urology*. Taylor & Francis Abingdon, Oxon UK
30. Delgado J, Berman JI, Maya C, Carson RH, Back SJ, Darge K (2019) Pilot study on renal magnetic resonance diffusion tensor imaging: are quantitative diffusion tensor imaging values useful in the evaluation of children with ureteropelvic junction obstruction? *Pediatr Radiol* 49(2):175–186
31. Hueper K, Gutberlet M, Rodt T et al (2011) Diffusion tensor imaging and tractography for assessment of renal allograft dysfunction—initial results. *Eur Radiol* 21(11):2427–2433
32. Lanzman RS, Ljimini A, Pentang G et al (2013) Kidney transplant: functional assessment with diffusion-tensor MR imaging at 3T. *Radiology* 266(1):218–225
33. Wang WJ, Pui MH, Guo Y, Wang LQ, Wang HJ, Liu M (2014) 3T magnetic resonance diffusion tensor imaging in chronic kidney disease. *Abdom Imaging* 39(4):770–775
34. Bedoya MA, Berman JI, Delgado J et al (2019) Relationship of renal apparent diffusion coefficient and functional MR urography in children with pelvicalyceal dilation. *Pediatr Radiol* 49(8):1032–1041. <https://doi.org/10.1007/s00247-019-04395-4>
35. Kataoka M, Kido A, Yamamoto A et al (2009) Diffusion tensor imaging of kidneys with respiratory triggering: optimization of parameters to demonstrate anisotropic structures on fraction anisotropy maps. *J Magn Reson Imaging* 29(3):736–744

Publisher's Note Springer Nature remains neutral with regard to jurisdictional claims in published maps and institutional affiliations.